Accepted for publication in AJ tentatively in the March issue

The Recent Star Formation History of NGC 5102[1]

Sylvie F. Beaulieu

Département de Physique, de Génie Physique et d'Optique and Centre de Recherche en Astrophysique du Québec (CRAQ), Université Laval, Québec, QC, G1V 0A6, Canada

sbeaulieu@phy.ulaval.ca

Kenneth C. Freeman

Research School of Astronomy and Astrophysics (RSAA), Australian National University, Cotter Road, Weston Creek, ACT 2611, Australia

kcf@mso.anu.edu.au

Sebastian L. Hidalgo

Instituto de Astrofísica de Canarias, Tenerife, Spain

shidalgo@iac.es

Colin A. Norman

Center for Astrophysical Sciences, Department of Physics and Astronomy, The Johns Hopkins University, Baltimore, MD 21218, USA

norman@stsci.edu

and

Peter J. Quinn

ICRAR, University of Western Australia, Crawley, WA, 6009, Australia

peter.quinn@uwa.edu.au

[1]Based on observations with the NASA/ESA *Hubble Space Telescope*, obtained at the Space Telescope Science Institute, which is operated by the Association of Universities for Research in Astronomy (AURA), Inc., under NASA Contract NAS 5-26555.

ABSTRACT

We present *Hubble Space Telescope* photometry of young stars in NGC 5102, a nearby gas-rich post-starburst S0 galaxy with a bright young stellar nucleus. We use the IAC-pop/MinnIAC algorithm to derive the recent star formation history in three fields in the bulge and disk of NGC 5102. In the disk fields, the recent star formation rate has declined monotonically and is now barely detectable, but a starburst is still in progress in the bulge and has added about 2% to the mass of the bulge over the last 200 Myr. Other studies of star formation in NGC 5102 indicate that about 20% of its stellar mass was added over the past Gyr. If this is correct, then much of the stellar mass of the bulge may have formed over this period. It seems likely that this star formation was fueled by the accretion of a gas-rich system with H I mass of about 2×10^9 $M_\odot$ which has now been almost completely converted into stars. The large mass of recently formed stars and the blue colours of the bulge suggest that the current starburst, which is now fading, may have made a significant contribution to build the bulge of NGC 5102.

Subject headings: galaxies: elliptical and lenticular - galaxies: starburst - galaxies: photometry - galaxies: evolution - galaxies: stellar content - galaxies: individual (NGC 5102)

1. Introduction

NGC 5102 is a low-luminosity galaxy of classic S0 appearance in the nearby Cen A group, at a distance of about 3.5 Mpc (van den Bergh 1976). Slightly smaller distances have been estimated by Karachentsev et al (2002) and Davidge (2008a), who note the potential effects of intermediate-age populations on the tip of the red giant distance. Table 1 summarises its basic parameters. Although it has the disk/bulge structure of a normal S0 galaxy (Pritchet 1979), NGC 5102 contains about 3×10^8 $M_\odot$ of H I (van Woerden et al. 1993[1]), an unusually bright nucleus dominated by young stars in optical light (Gallagher et al. 1975, van den Bergh 1976), and an extended distribution of ionized gas and dust in the inner regions of its bulge (McMillan et al 1994, Danks et al. 1979, Xilouris et al. 2004). A sprinkling of resolved stars from recent star formation is seen throughout its disk (van den Bergh 1976, Davidge 2008a).

[1]Values from the van Woerden et al. paper have been adjusted to our adopted distance through this paper.

It is not yet clear whether NGC 5102 is simply an S0 galaxy that has undergone a recent episode of star formation, or it is making a transition to the S0 state from a state more like a low-luminosity spiral (or vice versa; van Woerden et al. 1993; Davidge, 2008a). The formation of S0 galaxies is still poorly understood. We do not know how disk galaxies lose their interstellar medium to make the transition to the S0 state. With its S0 appearance and continuing low level of star formation, NGC 5102 may be a system caught in this transition phase, so we would like to understand the implications of its gas distribution and recent star formation history (SFH). One element in solving this problem is to delineate the recent SFH more precisely. Our main goal in this paper is to derive the history and amount of recent star formation in different regions of NGC 5102, particularly in the inner regions where the effects of the recent star formation are most visible.

The blue stellar nucleus of NGC 5102, with an absolute magnitude of M_V = -14.1, is significantly brighter than the typical nuclei of spiral galaxies (e.g., Böker et al. 2004). *IUE* spectra confirm the presence of early-type stars (Rocca-Volmerange & Guiderdoni 1987). The nucleus has an A-type absorption spectrum (Gallagher et al. 1975) and its colours (B-V = 0.2 and U-B = -0.1) are consistent with a single burst system of age 10^8 years and a mass of about 6×10^6 $M_\odot$ (Pritchet 1979). Our *Hubble Space Telescope* (*HST*) optical (WFPC2) and near-IR (NICMOS) images (to be discussed elsewhere) show that the nucleus is spatially unresolved: its FWHM is less than 3 pc. This is a compact configuration for such a bright stellar nucleus. We note that there is no evidence for current active galactic nucleus (AGN)-type nuclear activity from near-IR, optical, UV or X-ray spectra (Bendo & Joseph 2004; Gallagher et al 1975; Chandar et al 2004; Irwin et al. 2004).

Away from the nucleus, the B-V colours of the bulge and disk show a weak radial gradient, with B-V increasing with radius from about 0.65 in the bulge to about 0.75 in the disk (Pritchet 1979). The photometry of Sandage & Visvanathan (1978) shows that the mean $b-V$ and $V-r$ colours of the disk and bulge of NGC 5102 (between circular apertures of 15″ and 120″) are similar to the mean colours of Virgo S0 galaxies. The $u-V$ colour in this region of NGC 5102 is however at the blue extreme for these systems. These colours indicate the recent star formation superimposed on an older disk population. It appears that the effects of the recent star formation episode are widespread throughout NGC 5102, but are strongest in the inner regions. Direct evidence for an old population of stars in the outer disk comes from Davidge's (2008a) detection of red giants (see also Karachentsev et al 2002).

The H I in NGC 5102 is distributed in a ring of mass 2×10^8 $M_\odot$, radius 3.5 kpc and peak surface density 1.5 $M_\odot\,pc^{-2}$, with a central depression; the H I surface density rises again to about 0.9 $M_\odot\,pc^{-2}$ near its centre (van Woerden et al. 1993). Within this central depression,

McMillan et al. (1994) detected a prominent filament of ionized gas. The gas shows emission lines of [OI], [OII] and O[III], and is therefore unlikely to be photoionized; McMillan et al. favour shock excitation. Furthermore, from its expansion velocity, this filament appears to be younger ($\sim 10^7$ yr) than the nuclear stars, and McMillan et al. argued that they are probably not associated.

In summary, the H I ring, the presence of extended ionized gas within it, the active recent star formation in the inner bulge and the relatively long time since the most recent star formation event in the disk, suggest that we are seeing the effects of infall of gas rather than the burning out of a star-forming galaxy. This infall may have been in the form of a gas-rich galaxy, or of gas from the group environment. We note that most of the major galaxies in the Cen A group are disturbed in various ways (M83, Cen A, NGC 5253 and NGC 5102 itself) and several authors have suggested that gas from the group environment is responsible for these disturbances. This group gas has yet to be detected directly. A deep H I survey of the central regions of the Cen A group by de Blok et al. (2002) did not detect any new H I clouds; this survey was sensitive to clouds with H I masses greater than about 3×10^6 $M_\odot$. We also note that NGC 5102 is relatively isolated in the Cen A group (see Karachentsev et al 2002; Figure 1) and has no companions close enough to have recently interacted with it.

This paper presents the results obtained from observations using the *HST* WFPC2 detector (program 5400). We concentrate on the photometry of the PC fields only, because they were specifically positioned along the major axis of NGC 5102, and the PC chip, with its small pixel size, gives adequate signal-to-noise ratio (S/N) in the high surface brightness regions of NGC 5102. A future paper will address the stellar content, structure and dynamics of the nucleus.

2. WFPC2 Photometry

Three separate pointings of NGC 5102 were obtained with WFPC2 in the $B-$ and $V-$ band (F450W and F569W) in 1994 September and 1995 March. Table 2 gives details of the observing log. The fields were centred on the PC chip with the first field F1 positioned at the centre of NGC 5102, and then offset twice along the SW major axis of the galaxy so as to provide a field F2 in a transition region between the bulge and the disk (at radius $66''$), and then a field F3 in the disk (at $132''$). Figure 1 shows an overlay of the three PC positions on a Digitized Sky Survey (DSS) R image.

A background field was also obtained in order to estimate directly the contribution of

the Galactic background. Details on the position for each field are summarised in Table 3.

We used the F450W and F569W filters because they provided (in Cycle 4) satisfactory transformations to the standard BV system and they gave the best S/N for observations of our blue stars against the redder diffuse background of NGC 5102.

Figures 2, 3 and 4 show the WFPC2 PC images in the $V-$ band of the three fields. The PC chip has 800 x 800 pixels with a scale of $0''.0455$ pixel^{-1}. The detector was operating at $-88°$C in the low-gain setting of 7 e^- DN^{-1}. Instrumental parameters and in-orbit characteristics of WFPC2 can be found in Biretta et al. (1996).

The images were calibrated using the standard *HST* pipeline procedure and point-spread function fitting photometry was performed using HSTphot (Dolphin 2000a, Dolphin 2000b). The calibration includes corrections for charge transfer (in)efficiency (CTE), geometric distortion, aperture corrections , and zero-pointing. The total exposure time for each field in each filter is listed in column 5 of Table 3.

NGC 5102 has a very bright steep core and is severely affected by dust obscuration near its centre. The centre of NGC 5102 is saturated in both filters of our WFPC2 data within a $0''.5$ radius. In an attempt to map the dust lanes and patches in F1 and to facilitate the identification of stars, we used the IRAF[2] /STSDAS routines ELLIPSE and BMODEL in order to remove the background galaxy. Figure 5 shows the PC negative image of F1 with a smooth model subtracted. Results from the isophotal analysis, generated by the isophote fitting task ELLIPSE (Figures 6 and 7), show that the ellipticity of the galaxy increases gradually as the semimajor axis increases from the inner bulge to the surrounding disk, and the position angle of each fitted ellipses (excluding the inner $0''.5$ radius region) remains fairly constant. This confirms the results obtained by Williams & Schwarzschild (1979) and Pritchet (1979) that NGC 5102 shows no obvious twist.

In Figure 5 we can clearly see for the first time, in the central region of NGC 5102 (within $18''$ of the nucleus), the long-suspected dust lanes and patches, as well as the bright resolved stars from the starburst. McMillan et al. (1994) show an [OIII] λ5007 "difference" image of NGC 5102 over an extended region of $3' \times 5'$. The filamentary [OIII] emission extends over our two inner fields, although it cannot be seen in our broadband WFPC2 images. Figure 5 also shows the stars of F1 overlaid to illustrates our efforts to avoid using stars in the dusty regions and the messy and saturated central region within a radius of $0''.5$.

Colour-magnitude data for our three galaxy fields are shown in Figure 8 (left panels),

[2]IRAF is distributed by the National Optical Astronomy Observatories, which are operated by the AURA, Inc., under co-operative agreement with the National Science Foundation.

with their associated photometric errors (right panels). Only stars with magnitude errors ≤ 0.2 and a sharpness of ± 0.5 were retained. The colour-magnitude data for the background field F4 is shown in Figure 9. As mentioned earlier, the background field serves to measure the contribution from the local Galactic background. Here, we clearly see that contamination from background stars is not a serious problem.

We applied a Galactic extinction correction to the three galaxy fields using values of $A_B = 0.237$ and $A_V = 0.182$ from Schlegel et al. (1998). The central field has a fair amount of dust, as can be seen in Figure 5. We do not apply any extra reddening, as explained below, the uncertainty in reddening is absorbed in the derivation of the SFH, via a minimum χ^2 criterion. Overlaid on the CMDs are a series of $z = 0.02$ Padova Isochrones (F450W:Girardi et al. 2002; F569W: L. Girardi 2001, private communication); log(age) is shown next to each isochrone.

HSTphot has a routine to estimate the completeness of our photometry. A total of 590,000 artificial stars were distributed in the observed fields. Colours and magnitudes of the artificial stars were selected to sample the observed CMDs. The photometric list of artificial stars was derived exactly as for the original images.

The completeness as a function of colour for the V-band of our three fields is shown in Figure 10. The completeness shows a clear dependence on colour. Because of the high surface brightness and crowding in the inner field F1, the completeness limit is much brighter than in the outer fields F2 and F3.

3. Star Formation History

We now derive the SFH in the three fields from the stellar photometry. The SFH of NGC 5102 was obtained using the IAC-pop/MinnIAC algorithm (Aparicio & Hidalgo 2009). The method is based on the comparison of a synthetic CMD with the observed CMD by assuming that any SFH can be given as linear combination of simple stellar populations (SSPs). An SSP is defined by a set of stars with a small range in age and metallicity. The comparison is done by dividing the synthetic CMD in partial CMD models, each one composed by an SSP. The observed CMD and the synthetic CMD are gridding by defining a set of boxes on them. The SFH best matching the distribution of the stars in the CMDs is found using a chi-squared merit function. See Aparicio & Hidalgo (2009) for a detailed description of the method.

To build the synthetic CMD, we need to adopt a metallicity for NGC 5102. Davidge (2008a) derived the metallicity distribution function for the old red giants of the outer disk of

NGC 5102; he found that the metallicity ranges over the interval [M/H] = -0.9 to -0.1, with the distribution peaking near [M/H] = -0.6. As we will be estimating the SFH for relatively young stars, it seems appropriate to use the metallicity for the interstellar medium. The luminosity-metallicity relation of Tremonti et al. (2004) indicates an [O/H] value of about -0.2 (adopting a solar value of 12 + log(O/H) = 8.7). The compilation by Chandar et al. (2004) gives an [O/H] value of +0.3. We will adopt a solar metallicity $Z = 0.02$.

The method of Aparicio & Gallart (2004) was used to generate the synthetic CMD with a total of 600,000 stars. Girardi et al. (2000) stellar evolution library and bolometric corrections from Origlia & Leitherer (2000) were used. We adopted an initial mass function by Kroupa et al. (1993) with 20% of binary stars.

Observational errors were simulated in the synthetic CMD by using the result of the completeness tests (Figure 10). Only stars with a magnitude error smaller than 0.2 and corrected for Galactic extinction are used to derive the SFH (i.e., data from Figure 8).

An age binning of 20 Myr was selected for stars younger than 80 Myr. For older stars, a larger binning was selected. The CMDs were sampled with boxes of sizes 0.04 in colour and 0.2 in magnitude. We used 15 sets of SSPs to minimise the effect of the age sampling in the SFH. The sampling boxes in the CMDs were also shifted. This produced a set of solutions which were averaged and the average is adopted as the final SFH. The 1σ dispersion of the averaged solutions are used as error bars.

To minimise the uncertainties in the stellar evolution models, photometric zero-points, reddening and distance estimation, the SFHs were obtained by introducing different offsets in colour and magnitude in the CMD. The solution giving the minimum chi-squared was adopted as the best fit. This minimise the impact in the derivation of the SFH of poorly known variables whose effect is to shift the CMD. This is the case of the internal reddening mentioned in section 2. The technique finds the offsets that should be introduced to the CMD to obtain the SFH with the minimum chi-squared.

A note about the stability and uniqueness of the solution. The SFHs have been averaged by using different sampling parameters, which minimise the fluctuations in the SFH. This gives a solution which is stable independently of the age binning used. The uniqueness of the solution is related with the assumption made for the auxiliary functions used to build the synthetic CMD: initial mass function, metallicity, and binary fraction. If we assume that these functions are a good approximation of those present in the galaxy, then our solution can be consider as unique. A detailed discussion about the stability and uniqueness of the solutions provided by IAC-pop/MinnIAC can be found in Aparicio & Hidalgo (2009).

Figures 11-16 present the SFH and CMDs (observed and solved) for our three fields.

The CMD of the bulge field F1 (Figure 8) shows a history of recent star formation. The isochrones in Figure 8 show that stars as young as 10^7 years are present. By comparing the dereddened CMD of F1 with the synthetic CMD (Figure 12), we can make a quantitative estimate of the SFH. In Figure 11, we show the SFH of the central field F1. Because of the relatively bright background (and thus of the completeness limit), we cannot estimate the SFH in F1 for stellar ages greater than about 200 Myr. The star formation rate appears to have been relatively high over the past 20 Myr, in contrast to the two disk fields F2 and F3 (note that the vertical scales in Figures 11, 13, and 15 are not all the same).

For the inner disk field F2, we present the observed and synthetic CMDs in Figure 14. In this field, the SFH (Figure 13) shows a decline in the star formation rate from about 0.5 Gyr; the past 200 Myr appear to have been quiescent.

We show the observed and synthetic CMDs for the disk field F3 in Figure 16, and the SFH in Figure 15. The star formation rate has declined smoothly from about 200 Myr ago, and has been quiescent over the past 40 Myr.

4. Discussion and Conclusion

We have measured the recent SFH of three fields in NGC 5102: the inner bulge, inner disk and disk. In the two outer fields, the SFH is qualitatively similar, showing a declining star formation rate with no detectable star formation in the past 40 Myr. In the innermost field, the star formation rate has been more or less constant over the past 200 Myr, but with an abrupt burst in the past 20 Myr. This is all consistent with the earlier data from colours and integrated spectra. What can we conclude about the nature of NGC 5102: is it a system that has recently made the transition to the S0 state, or are we simply seeing the after-effects of a star formation event fueled by the ring of H I that lies only a few kpc from the centre ? How much stellar mass was involved in this star-forming episode, and is it a significant fraction of the total stellar mass of NGC 5102 ?

First we estimate the present stellar mass of NGC 5102. This galaxy has a strong colour gradient (e.g. Pritchet 1979), so its M/L ratio changes significantly with radius. We adopt the B-band surface brightness profile given by van Woerden et al (1993). When integrated over radius, after adjusting the surface brightness of the disk for inclination (line of sight effect only, no internal extinction correction), this profile gives an apparent B magnitude of 10.34, in excellent agreement with the RC3 value in Table 1. The disk and the bulge provide about 60% and 40% of the total light respectively. To calculate the radial change of M/L, we use the B-R data of Pritchet (1979) and Persson et al. (1979) which extend to a

radius of about 60 arcsec, and assume that the unreddened colour $(B\text{-}R)_\circ$ remains constant at 1.50 at larger radii. We then use the models of Bell & de Jong (2001; excluding the closed box and dynamical time models which they regard as implausible) to derive the local $M/L_{\rm B}$ value from the $(B\text{-}R)_\circ$ colour at each radius. Integrating the stellar surface density over the galaxy for each of the models gives a mean total stellar mass of $(5.6 \pm 0.8) \times 10^9$ $M_\odot$, where the error shows the scatter between the models. This is in good agreement with Davidge"s (2008a) dynamical estimate of 7×10^9 $M_\odot$.

We now assume that the SFH is axisymmetric, and integrate the star formation rates shown in Figures 11, 13, and 15 over the region of NGC 5102, sampled by our three fields. For F2 and F3, we are therefore deriving the star formation rates integrated over annuli around NGC 5102 with the width and mean radius of these two fields. To integrate the mass of stars formed, we first need the mass of recently formed stars per unit area of the stellar disk. The observed star formation rates shown in Figures 11, 13, and 15 are per unit area on the sky, so the surface density of stars formed must be corrected for the inclination of NGC 5102. We derive an inclination of 66° (face-on is 0°) using axial ratios measured at several isophote levels in the outer disk from the DSS R-band image of NGC 5102 and assuming an intrinsic axial ratio of 0.2 for the disk. The mean surface densities of newly formed stars in each field are given in Table 4: Column 1 is the field, Column 2 is the surface density of new stars, and Column 3 shows the total mass of stars formed over the past 200 Myr in F1 itself and in the annuli associated with F2 and F3 as described above. Column 4 shows the time interval over which the star formation rate was integrated.

For the disk, the mass is about 60% of the total stellar mass or 3.3×10^9 $M_\odot$. The annuli associated with the disk fields F2 and F3 cover about half of the disk area visible in Figure 1. Assuming that the star formation rate in F2 and F3 is typical of the disk, then from Table 4 the mass of new stars formed in the disk over the past 200 Myr is about 2×10^6 $M_\odot$. This represents less than 0.1% of the disk mass. We conclude that the star formation observed in the disk over the past 200 Myr has contributed negligibly to build up the disk. On the other hand, Davidge (2008a) concludes that at least 20% of the stellar disk mass was formed in the past Gyr. If both of these inferences are correct, then it seems clear that the mean star formation rate in the period between 200 Myr and 1 Gyr ago was about 80 times higher than the rate which we have derived. We are seeing the disk near the end of its recent starburst.

For the bulge, the mass is about 40% of the total or 2.2×10^9 $M_\odot$. Our F1 covers roughly half of the bulge area visible in Figure 1, so the mass of new stars formed in the bulge over the past 200 Myr is about 4×10^7 $M_\odot$. The $B\text{-}R$ colour profile derived by Pritchet (1979) is approximately constant within the bulge, outside of the nuclear region, so we assume that

the star formation rate per unit area in F1 is representative of the entire bulge area. Then the star formation events of the past 200 Myr have contributed about 2% of the stellar mass of the bulge.

Although we have no direct information about the star formation rate in the bulge at earlier times, this 2% growth in the last 200 Myr is interesting. It would not take a very large enhancement of this rate over the previous Gyr to add a substantial amount of stars to the bulge. For example, a sixfold increase in the mean star formation rate in the bulge over the period between 200 Myr and 1 Gyr ago would be enough to double the stellar mass of the bulge in the last Gyr. This sixfold increase is much less than the increase in the disk star formation rate over the same period inferred above.

Continuing with this argument, we note that the SFH of F1 (Figure 11) shows a gradual decay in the star formation rate from 200 Myr ago, a brief enhancement about 70 Myr ago and a very recent star formation episode in the last 20 Myr. The SFH from 200 Myr to 20 Myr ago can be represented by an exponential decay with a timescale of 110 Myr, plus the enhancement at 70 Myr ago. The decaying exponential component contributed about 2.2×10^7 $M_\odot$ of stars to the bulge over the last 200 Myr, with the remainder coming from the two short-duration bursts. Extrapolating this exponential SFH backward in time, we would need to go back only 700 Myr ago for this starburst to generate the entire stellar mass of the bulge. If the starburst did indeed start its exponential decay 700 Myr ago, the instantaneous star formation rate of the exponential component at that time would have been about 20 $M_\odot\,yr^{-1}$, compared with the mean rate of about 0.1 $M_\odot\,yr^{-1}$ over the past 200 Myr.

What is the likely scenario for the evolution of NGC 5102 ? The colours of the outer disk are similar to those of present-day S0 galaxies in the Virgo cluster (see Section 1), indicating that the starburst is superimposed on an older disk population. From Davidge's (2008a) argument, the starburst appears to have been very substantial, and we can probably exclude the possibility that the residual star formation seen now is the remains of the normal star formation of a spiral galaxy exhausting its gas and making a passive transition to an S0 galaxy.

Before the starburst, NGC 5102 would have been a dwarf disk galaxy with a stellar mass of about 4×10^9 $M_\odot$, and an absolute magnitude of about $M_B = -17$. The outer regions of NGC 5102 appear to be relatively unaffected by the starburst, and the surface brightness profile shown by van Woerden et al. (1993) indicates an outer disk of normal surface brightness (e.g., Freeman 1970). NGC 5102 then captured a gas cloud or gas-rich galaxy with an H I mass of at least 2×10^9 $M_\odot$ which fueled the starburst and added about 20% to the existing stellar mass, mainly in the bulge. The idea of capture of a gas cloud is not novel in the context of the Cen A group: similar captures have been invoked to explain

the starburst in NGC 5253 and the disturbed structure of M83 and Cen A itself (e.g., López-Sánchez et al, 2008). At the peak of its recent star formation activity, NGC 5102 may have looked rather like the dwarf starburst system M82 (e.g., Mayya et al. 2006; Davidge 2008b). Now we see it in a late phase of the star formation event, as an S0 galaxy with the star formation rate close to zero and the gas almost exhausted: the residual HI mass is about 3×10^8 $M_\odot$ and the mass of ionised gas is only about 9×10^5 $M_\odot$ (McMillan et al 1994).

This picture of star formation driven by infalling gas from the observed neutral hydrogen is supported by the similarity of dynamical and star formation timescales, all around 30 Myr, for NGC 5102. We list some of the relevant timescales below.

(i) McMillan et al (1994) discovered a prominent filament of ionized gas extending roughly from the centre of the galaxy in both directions along the major axis of the galaxy which they argue is excited by a low velocity shock. The velocity gradient along this feature has an associated timescale of about 20 Myr, comparable with the age of the most recent star-forming event in our field F1.

(ii) The measured HI rotation curve extends inwards to a radius of 2 kpc. At this radius the rotation period is about 160 Myr (van Woerden et al 1993) so the infall time (typically 0.2 × rotation period) is about 30 Myr.

(iii) Although the decay timescale of the star formation rate in F1 is longer (about 110 Myr), the SFH shows superimposed events with shorter timescales of about 20 Myr.

(iv) In our disk field (F3), the SFH shown in Figure 15 can again be well represented by an exponential decay, with a timescale of 58 Myr. As in F1, the SFH shows a brief enhancement about 70 Myr ago. The HI infall time at the radius of F3 is about 40 Myr.

There are two important classes of cosmological galaxy formation models that can apply to this interpretation of NGC 5102. Both of them may have been active in the case of NGC 5102, and it is worthwhile to discuss them here and point out how their relative significance might be determined.

(I) The density and velocity fields of gas in galaxies at redshift ≈ 2 (where the peak of the star formation in the universe occurs) appear clumpy and turbulent. In the remarkable SINFONI observations from Genzel and colleagues (Forster-Schreiber et al 2009; Shapiro et al. 2009; Burkert et al. 2009) one sees a small number of massive clumps. Now, the relaxation time for a clumpy disk with N clumps is $T_R \sim NT_d$ where T_d is the dynamical time. In this picture then, once a clump is released from the HI disk and sent toward the central region, the timescale would be T_d and the time in between such events would be $T_R \sim 3 - 10\ T_d$ (assuming there are 3 -10 clumps). Thus, a secular bulge building process

can occur in such disks. Recent interesting theoretical models of Birnboim et al (2007), Dekel et al (2009a & 2009b), and Ceverino et al (2009) may also apply to cold (HI) clumpy turbulent HI distributions and flows as discussed here.

(II) The classic starburst feedback ideas that apply to downsizing and quenching of the galaxy formation process in many available feedback models involve halting the formation of galaxies by feedback processes. In the case of NGC 5102, one would imagine the following cycle. The HI distribution builds up in the centre and then a threshold is reached where at least part of the central HI mass becomes dynamically unstable and a starburst results on the dynamical timescale. Then a starburst wind (or in some cases an AGN generated feedback process) is triggered, the remaining gas is then blown away and the star formation process is halted. The central region is then replenished on a timescale which is something like the turbulent-velocity crossing time of the central region − in the case of NGC 5102, one has a turbulent velocity of say $V_t \sim 10$ km s^{-1} and a scale of $R_B \sim 1$ kpc, resulting in a refilling time - during which the star formation is effectively quenched - of $T_q \sim 100$ Myr. We do not see the feedback process of the starburst driven wind in NGC 5102, but we do see the large scale ionised gas shell that it may have formed.

How to estimate the relative importance of these two scenarios in the case of NGC 5102 ? (1) The HI map needs to be repeated with significantly higher spatial resolution. The question of HI clumpiness is important to resolve. Similarly, molecular (CO) observations are also essential. (2) The details of the possible feedback from the shell structure and other associated gas are now most interesting and new deep X-ray and spectroscopic studies would be the best way to proceed. (3) Detailed kinematic data on the bulge of NGC 5102 might help determine if there were randomly distributed blobs falling in to make the bulge, or a more quiescent picture of central disk refilling.

Sorting out the relationship between the higher redshift, $z \sim 2$, observations and this excellent local laboratory for bulge formation provides a rare opportunity

It would be interesting to know whether the bulge of NGC 5102 was primarily built during the recent starburst. To the level at which we can work here, this cannot be excluded. As a test of this possibility, it would be useful to search for older stars in the bulge: this is probably best done with adaptive optics or *HST* imaging in the near-IR, to detect the tip of the old (> 1 Gyr) red giant branch against the bright background of the bulge. A negative outcome of such a search for old bulge stars in NGC 5102 would suggest that its bulge was indeed primarily built up in this one recent and brief star-forming event.

Such rapid formation of a bulge at a relatively recent epoch would be a different mode of bulge formation from the more usual scenarios of forming classical and pseudo bulges in

disk galaxies (e.g. Kormendy & Kennicutt 2004). NGC 5102 is a low-luminosity S0 system. Even if its bulge turns out to have formed in a single recent event, one cannot generalise its SFH to more luminous S0 galaxies in general. However we are tempted to ask whether this kind of rapid bulge formation, driven by infall and starbursts at later and maybe multiple epochs, could be more common in S0 galaxies with their relatively quiescent disks. If so, it may be at least part of the reason why S0 galaxies have predominantly larger bulges than spirals (e.g., Dressler 1980).

We are grateful to Leo Girardi for providing the unpublished set of isochrones for *HST*/WFPC2 F569W. SFB thank J. Gallagher and C. Pritchet for fruitful discussions. We thank the referee for helpful comments which improved the presentation of the paper. This study was partly funded by NASA grant HST-GO-07455.01-96A. This research has made use of the NASA/IPAC Extragalactic Database (NED) which is operated by the Jet Propulsion Laboratory, California Institute of Technology, under contract with the National Aeronautics and Space Administration. This research has made use of NASA's Astrophysics Data System Bibliographic Services, and of photographic data obtained using the UK Schmidt Telescope. The UK Schmidt Telescope was operated by the Royal Observatory Edinburgh, with funding from the UK Science and Engineering Research Council, until 1988 June, and thereafter by the Anglo-Australian Observatory. The Digitized Sky Survey was produced at the Space Telescope Science Institute under US Government grant NAG W-2166. To produce some of the figures, we used the KARMA package (Gooch 1997).

REFERENCES

Aparicio, A., & Gallart, C. 2004, AJ, 128, 1465

Aparicio, A., & Hidalgo, S.L. 2009, AJ, 138, 558

Bell, E.F. & de Jong, R.S. 2001, ApJ, 550, 212

Bendo, G. J., & Joseph, R. D. 2004, AJ, 127, 3338

Biretta, J., et al. 1996, WFPC2 Instrument Handbook (version 4.0; Baltimore:STScI)

Birnboim, Y., Dekel, A., & Neistein, E. 2007, MNRAS 380, 339

Böker, T., Sarzi, M., McLaughlin, D. E., van der Marel, R. P., Rix, H.-W., Ho, L. C., Shields, J. C. 2004, AJ, 127, 105

Burkert, A. et al.2009 arXiv 0907.4777

Ceverino, D., Dekel, A. & Bournaud, F. 2009, ArXiv 0907.3271

Chandar, R., Leitherer, C., & Tremonti, C. A. 2004, ApJ, 604, 153

Danks, A. C., Lausten, S. & van Woerden, H. 1979, A&A, 73, 247

Davidge, T.J. 2008a, AJ, 135, 1636

Davidge, T.J. 2008b, AJ, 136, 2502

de Blok, W.J.G., Zwaan, M.A., Dijkstra, M., Briggs, F.H. & Freeman, K.C. 2002 A&A, 382, 43

Dekel, A., Sari, R., & Ceverino, D. 2009b, 2009b, ApJ, 703, 785

Dekel, A. et al 2009a, Nature 457, 451

Dolphin, A.E. 2000a, PASP, 112, 1383

Dolphin, A.E. 2000b, PASP, 112, 1397

Dressler, A. 1980, ApJ, 236, 351

Forster-Schreiber, N.M. et al 2009, ApJ, 706, 1364

Freeman, K. 1970, ApJ, 160, 811

Gallagher, J., Faber, S., & Balick, B. 1975, ApJ, 202, 7

Girardi, L., Bertelli, G., Bressan, A., Chiosi, C., Groenewegen, M.A.T., Marigo, P., Salasnich, B., & Weiss, A. 2002, A&A, 391, 195

Girardi, L., Bressan, A., Bertelli, G., & Chiosi, C. 2000, A&AS, 141, 371

Gooch, R.E. 1997, PASA, 14, 106

Irwin, J.A., Bregman, J.N., Athey, A. E. 2004, ApJ, 601, 143

Karachentsev, I.D, et al. 2002, A&A, 385, 21

Koribalski et al. 2004, AJ, 128, 16

Kormendy, J. & Kennicutt, R.C. 2004, ARAA, 42, 603

Kroupa, P., Tout, C.A., & Gilmore, G. 1993, MNRAS, 262, 545

López-Sánchez, A., Koribalski, B.,Esteban, C., Garcia-Rojas, J. 2008, Galaxies in the Local Volume, Astrophysics and Space Science Proceedings, Volume . ISBN 978-1-4020-6932-1. Springer Netherlands, 2008, p. 53

Mayya, Y.D., Bressan, A., Carrasco, L., & Hernadez-Martinez, L. 2006, ApJ, 649, 172

McMillan, R., Ciardullo, R., & Jacoby, G. H. 1994, AJ, 108, 1610

Origlia, L. & Leitherer, C. 2000, AJ, 119, 2018

Persson, S.E., Frogel, J.A. & Aaronson, M. 1979, ApJS, 39, 61

Pritchet, C. 1979, ApJ, 231, 354

Rocca-Volmerange, B., & Guiderdoni, G. 1987, A&A, 175, 15

Sandage, A. & Visvanathan, N. 1978, ApJ, 273, 707

Schlegel, D.J., Finkbeiner, D.P., & Davis, M. 1998, ApJ, 500, 525

Shapiro, K. et al. 2009, 7 pages, to appear in the proceedings of "Galaxy Evolution: Emerging Insights and Future Challenges," Austin, TX, 11-14 Nov 2008

Tremonti, C.S., et al. 2004, ApJ, 613, 898

van den Bergh, S. 1976, AJ, 81, 795

van Woerden, H., van Driel, W., Braun, R., & Rots, A. H. 1993, A&A, 269, 15

Williams, T. B., & Schwarzschild, M. 1979, ApJ, 227, 56

Xilouris, E. M., Madden, S. C., Galliano, F., Vigroux, L., & Sauvage, M. 2004, A&A, 416, 41

Table 1. Basic Parameters for NGC 5102

Parameter	Value	Notes
R.A. (J2000.0)	13 21 57.6	1
decl. (J2000.0)	−36 37 49	1
Morphological type	SA0	1
Adopted distance (Mpc)	3.5	
Distance modulus $(m-M)_o$	27.72	
Helio radial velocity (km s^{-1})	468	1,2
Major diameter (arcmin)	8.7	1
Minor diameter (arcmin)	2.8	1
Inclination (deg)	66	
P.A. major axis (deg)	48	3
M_{HI} ($M_\odot$)	2×10^8	4
M_{HI}/L_B^0 ($M_\odot/L_\odot$)	0.12	4
[Fe/H]	0.0	5
Reddening $E(B-V)$	0.055	1
Total B magnitude B_T	10.35	3
$(B-V)_T$	0.72	3

References. — (1) NED; (2) Koribalski et al. 2004; (3) RC3; (4) van Woerden et al. 1993 with the M_{HI} adjusted to our adopted distance; (5) refers to the young population

Table 2. *HST*/WFPC2 Data Sets for NGC 5102 : *HST* Program 5400

Data Set	Filter	Field	Date	Exposure (s)
u2bt0101t	F450W	1	1994 Sep 2	400
u2bt0102t	F450W	1	1994 Sep 2	400
u2bt0103t	F450W	1	1994 Sep 2	400
u2bt0104t	F450W	1	1994 Sep 2	400
u2bt0105t	F450W	1	1994 Sep 2	400
u2bt0106t	F450W	1	1994 Sep 2	400
u2bt0107t	F450W	1	1994 Sep 2	400
u2bt0108t	F450W	1	1994 Sep 2	400
u2bt0109t	F569W	1	1994 Sep 2	500
u2bt010at	F569W	1	1994 Sep 2	500
u2bt010bt	F569W	1	1994 Sep 2	500
u2bt010ct	F569W	1	1994 Sep 2	500
u2bt010dt	F569W	1	1994 Sep 2	500
u2bt010et	F569W	1	1994 Sep 2	500
u2bt010ft	F569W	1	1994 Sep 2	500
u2bt010gt	F569W	1	1994 Sep 2	500
u2bt010ht	F450W	2	1994 Sep 2	1100
u2bt010it	F450W	2	1994 Sep 2	1100
u2bt010jt	F450W	2	1994 Sep 2	1100
u2bt010kt	F569W	2	1994 Sep 2	1100
u2bt010lt	F569W	2	1994 Sep 2	1100
u2bt010mt	F569W	2	1994 Sep 2	1100
u2bt0201t	F450W	3	1994 Sep 8	1100
u2bt0202t	F450W	3	1994 Sep 8	1100
u2bt0203t	F450W	3	1994 Sep 8	1100
u2bt0204t	F569W	3	1994 Sep 8	1100
u2bt0205t	F569W	3	1994 Sep 8	1100
u2bt0206t	F569W	3	1994 Sep 8	1100
u2bt0301t	F450W	4	1995 Mar 20	1100
u2bt0302t	F450W	4	1995 Mar 20	1100
u2bt0303t	F450W	4	1995 Mar 20	1100

Table 2—Continued

Data Set	Filter	Field	Date	Exposure (s)
u2bt0304t	F569W	4	1995 Mar 20	1100
u2bt0305t	F569W	4	1995 Mar 20	1100
u2bt0306t	F569W	4	1995 Mar 20	1100

Table 3. *HST*/WFPC2 PC Positions

Field	R.A., Decl. (J2000.0)	Position	P.A.	Total Exp. (s)
1	13 21 57.9 − 36 37 49.0	centre	$176^o.76$	F450W = 3200
				F569W = 4000
2	13 21 54.2 − 36 38 39.1	66″ SW	$176^o.76$	F450W = 3300
				F569W = 3300
3	13 21 49.9 − 36 39 20.1	132″ SW	$180^o.56$	F450W = 3300
				F569W = 3300
4	13 22 23.7 − 36 37 18.4	Backgrd		F450W = 3300
				F569W = 3300

Table 4. Derived Star Formation Densities and Masses

Field	Mean SFD ($M_\odot\,pc^{-2}$)	Stellar Mass ($M_\odot$)	Time Interval (Myr)
F1	30	2.1×10^7	0 - 200
F2	0.003	1.3×10^4	0 - 200
F3	0.11	1.0×10^6	0 - 200

Note. — Note. See the text for explanation

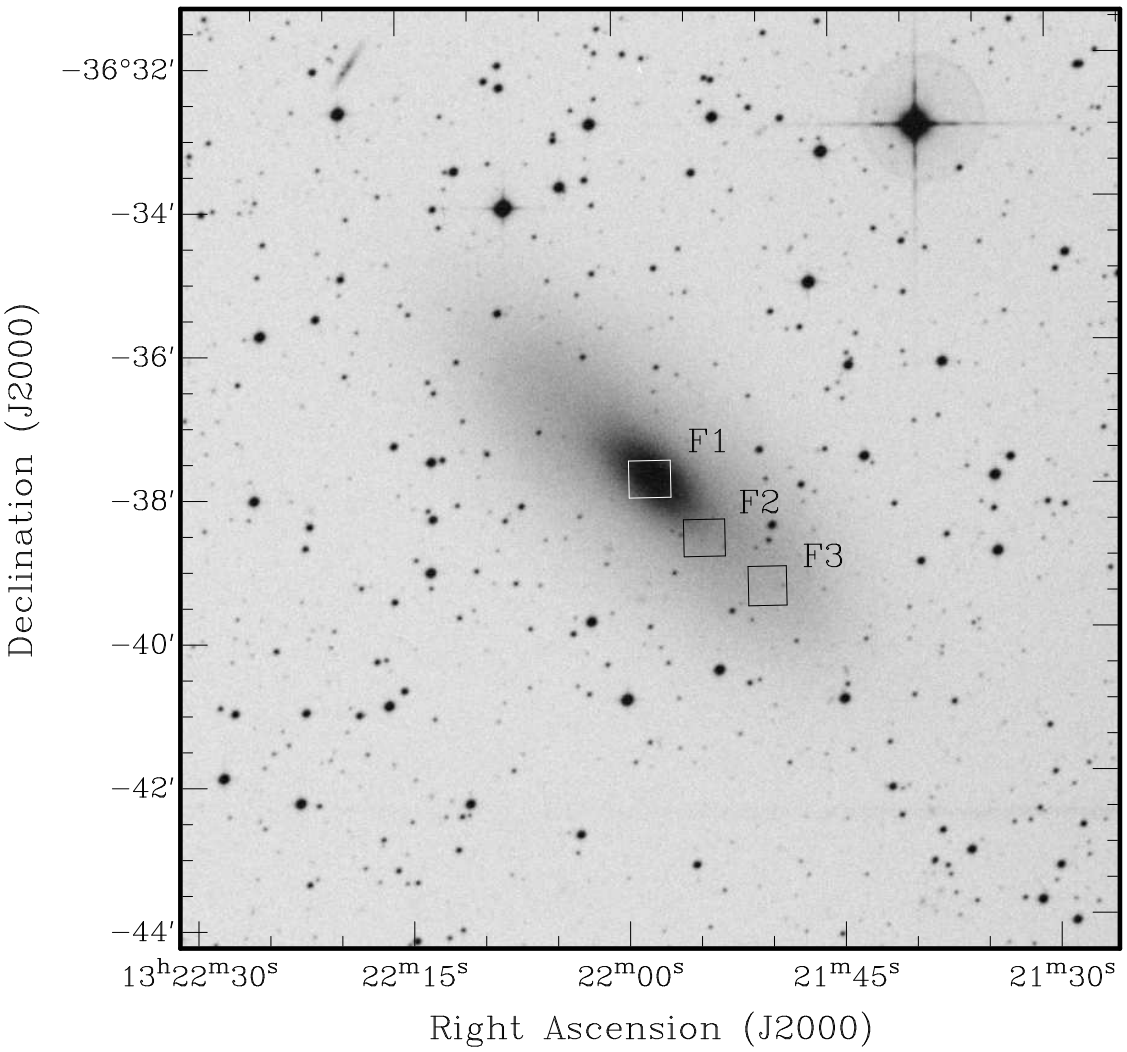

Fig. 1.— DSS2 R-band image of NGC 5102 showing the position of the three WFPC2 PC fields.

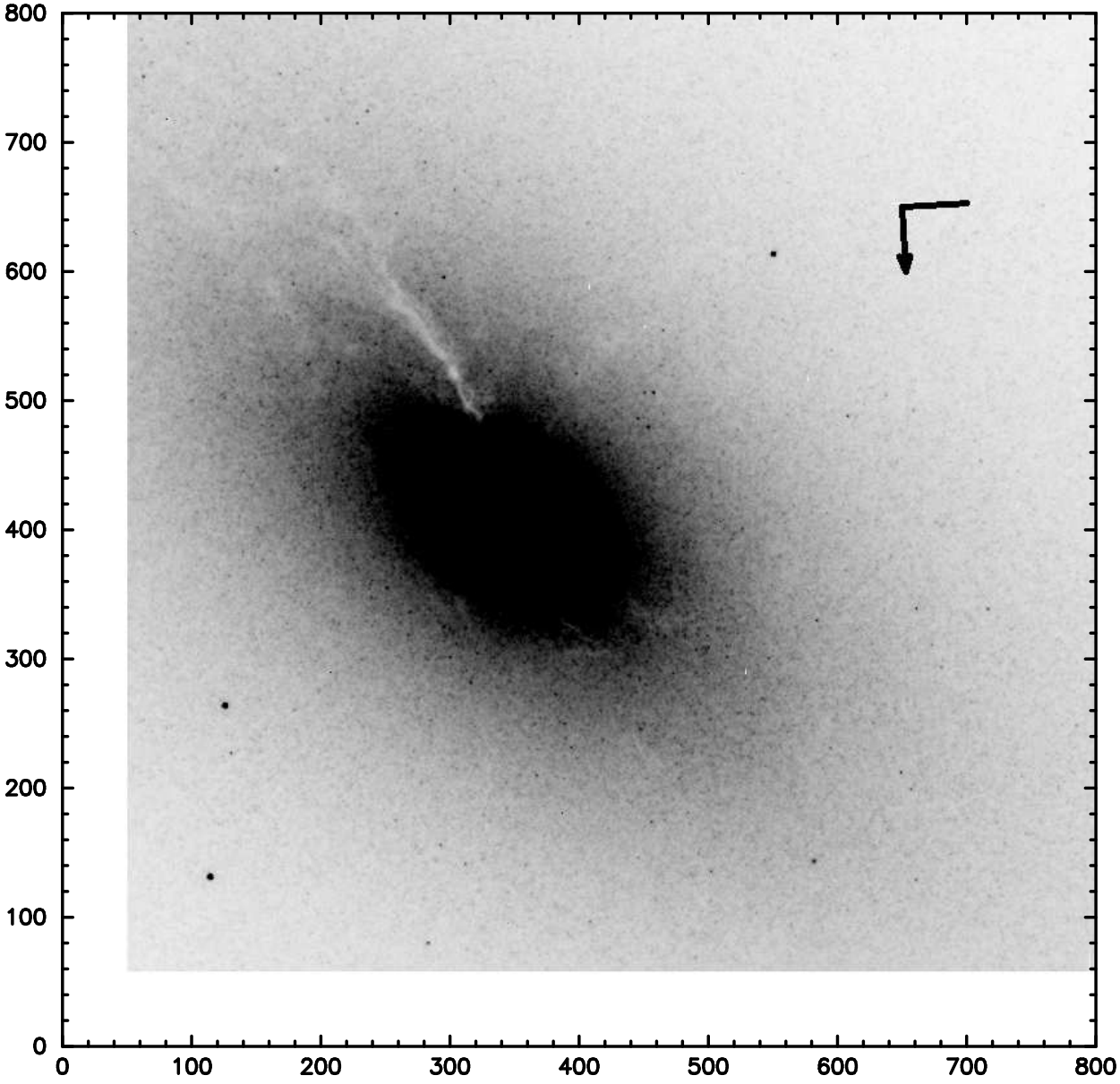

Fig. 2.— *HST*/WFPC2 PC image in the V- band for the centre of NGC 5102 (field 1). The arrow points to the north. The PC chip has 800 x 800 pixels with a scale of $0''.0455$ pixel^{-1}. The CCD characteristics are the same for Figures 2, 3 and 4.

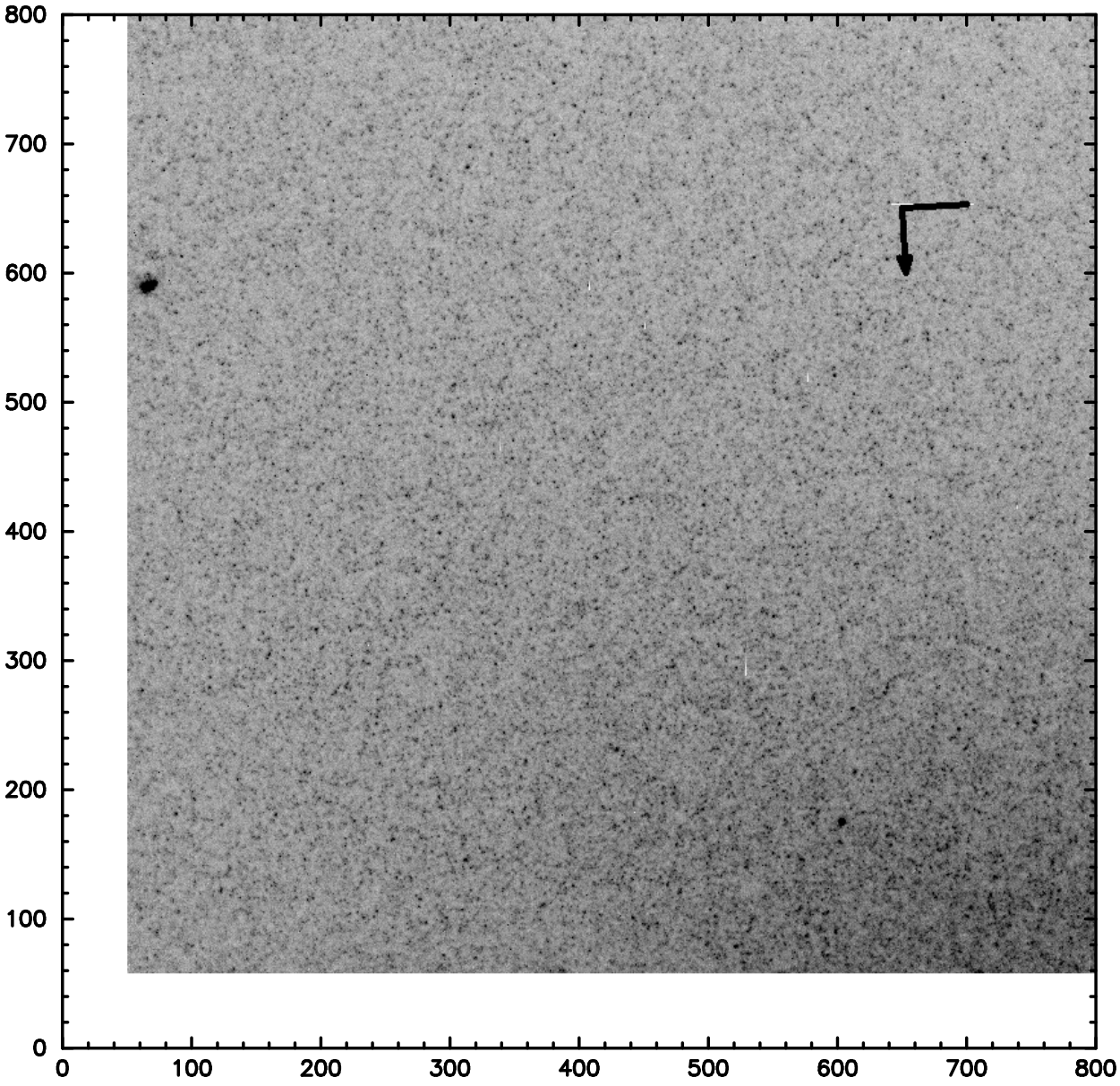

Fig. 3.— *HST*/WFPC2 PC image in the V- band for the intermediate position (field 2) of NGC 5102. The bright resolved stars are visible.

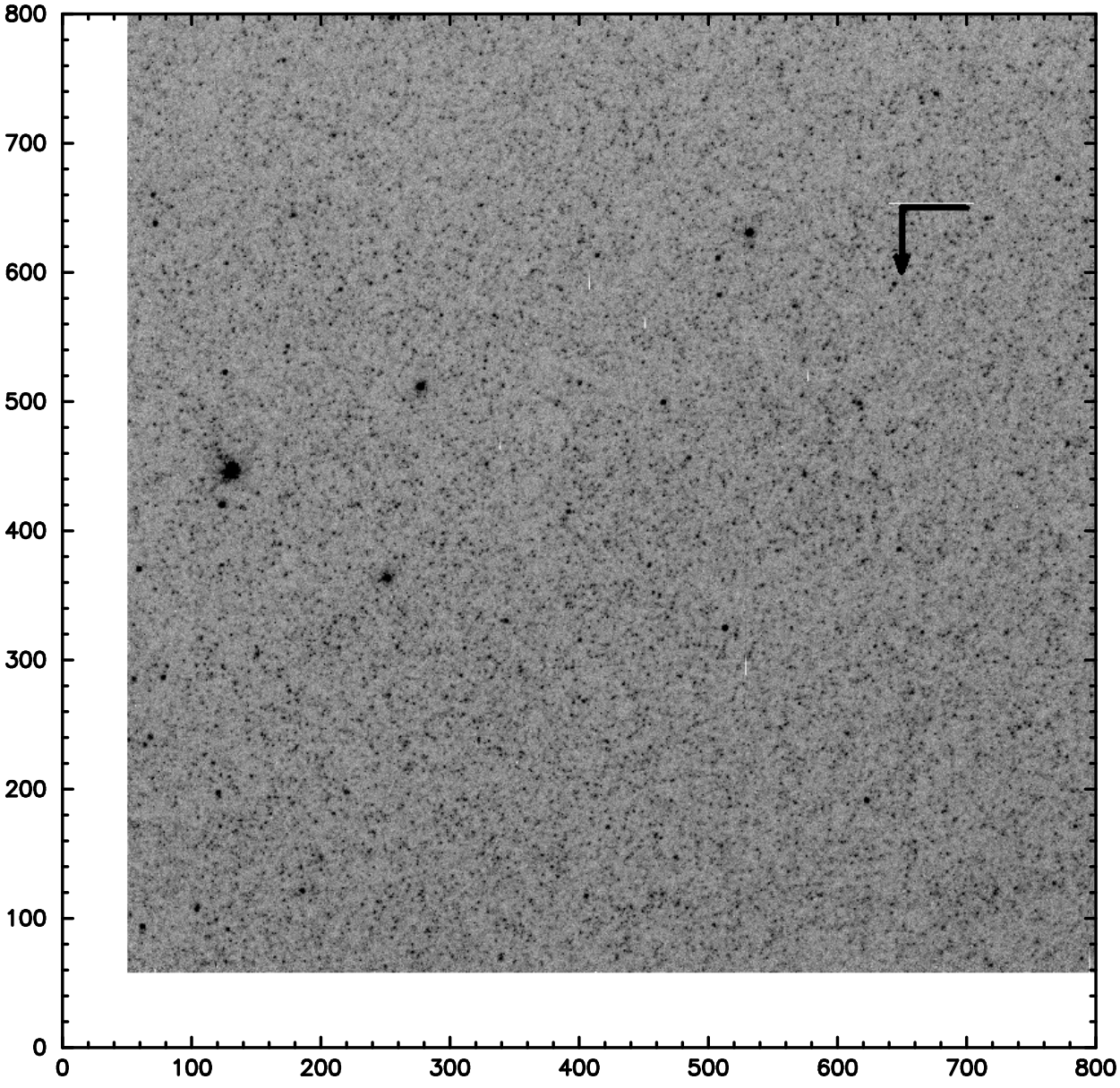

Fig. 4.— *HST*/WFPC2 PC image in the V- band for the disk field (field 3) of NGC 5102.

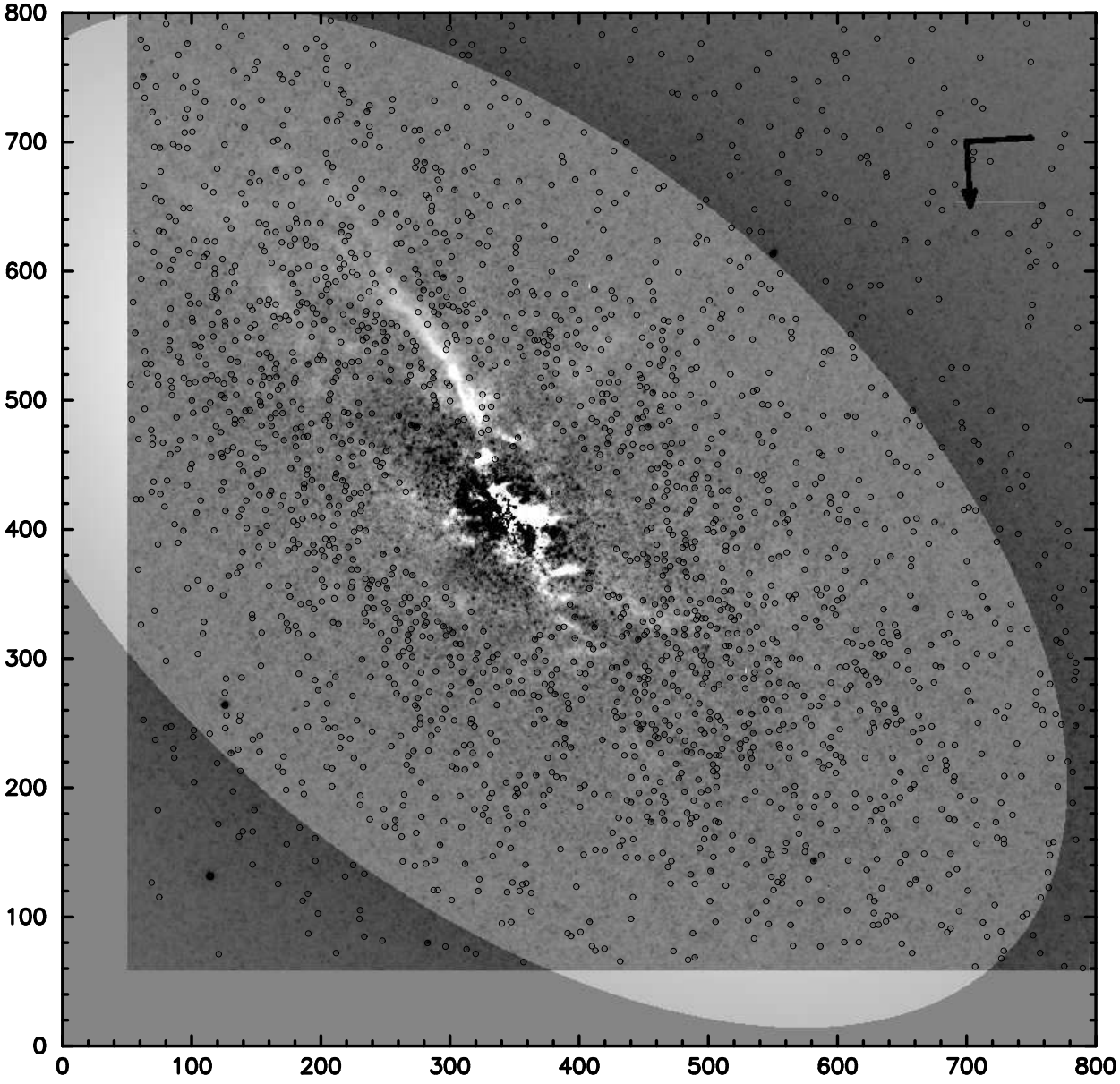

Fig. 5.— *HST*/WFPC2 PC negative image of the inner (12″ x 12″) region of NGC 5102 (field 1) with a smooth model subtracted. The dust lanes and patches, as well as the bright resolved stars from the starburst are clearly visible. Overlaid are the detected stars.

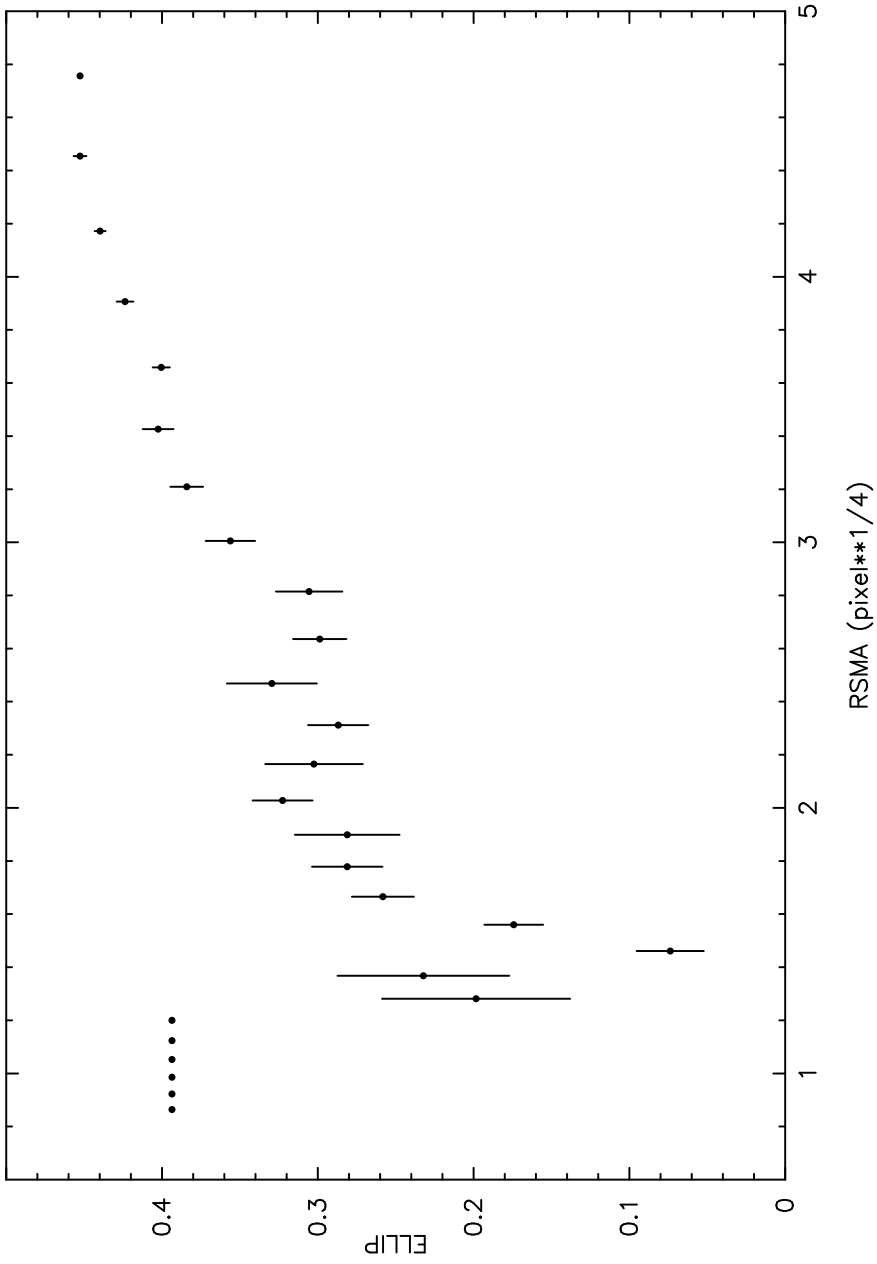

Fig. 6.— Semimajor axis vs. the ellipticity from the smooth model.

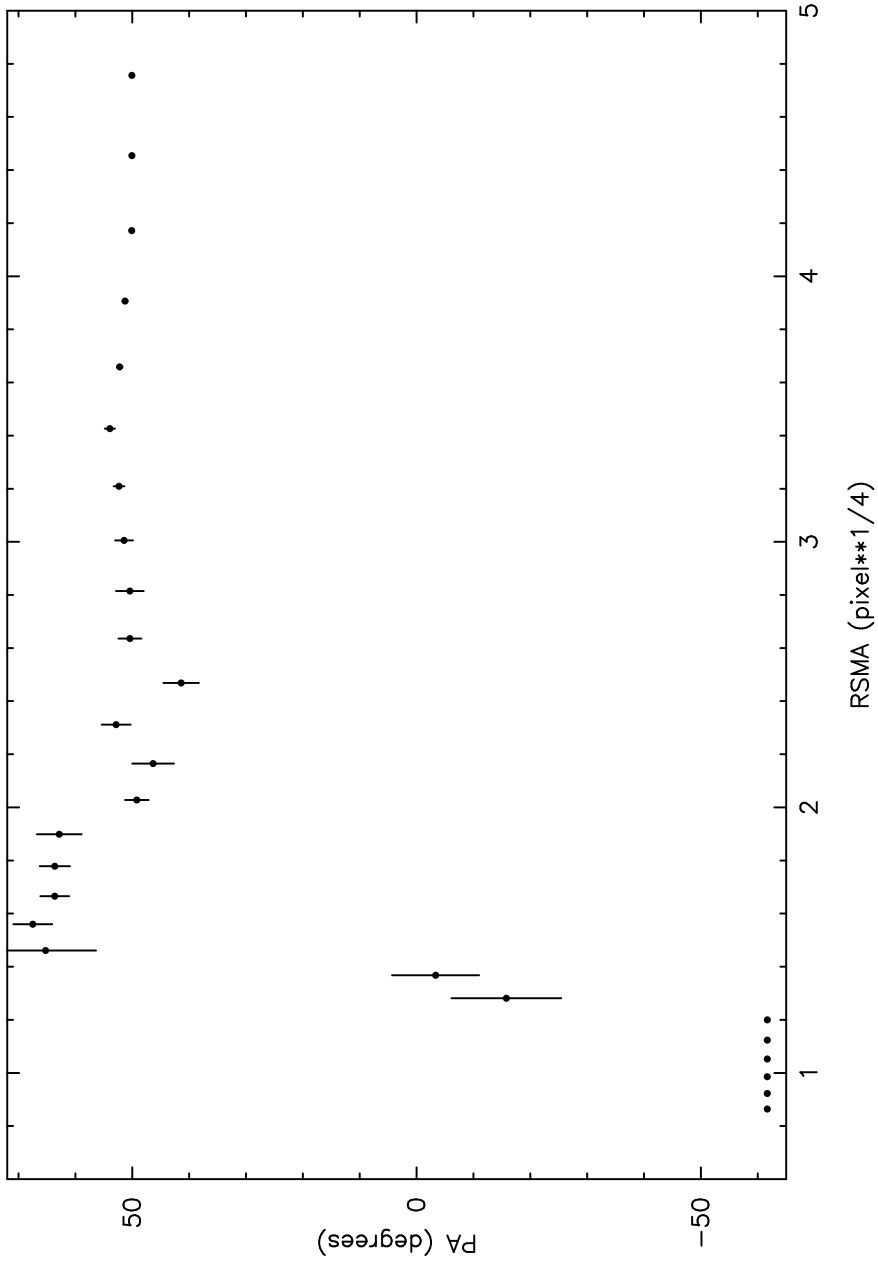

Fig. 7.— Semimajor axis vs. the position angle from the smooth model. The position angle of each fitted ellipses (excluding the inner $0''.5$ radius region) remains fairly constant.

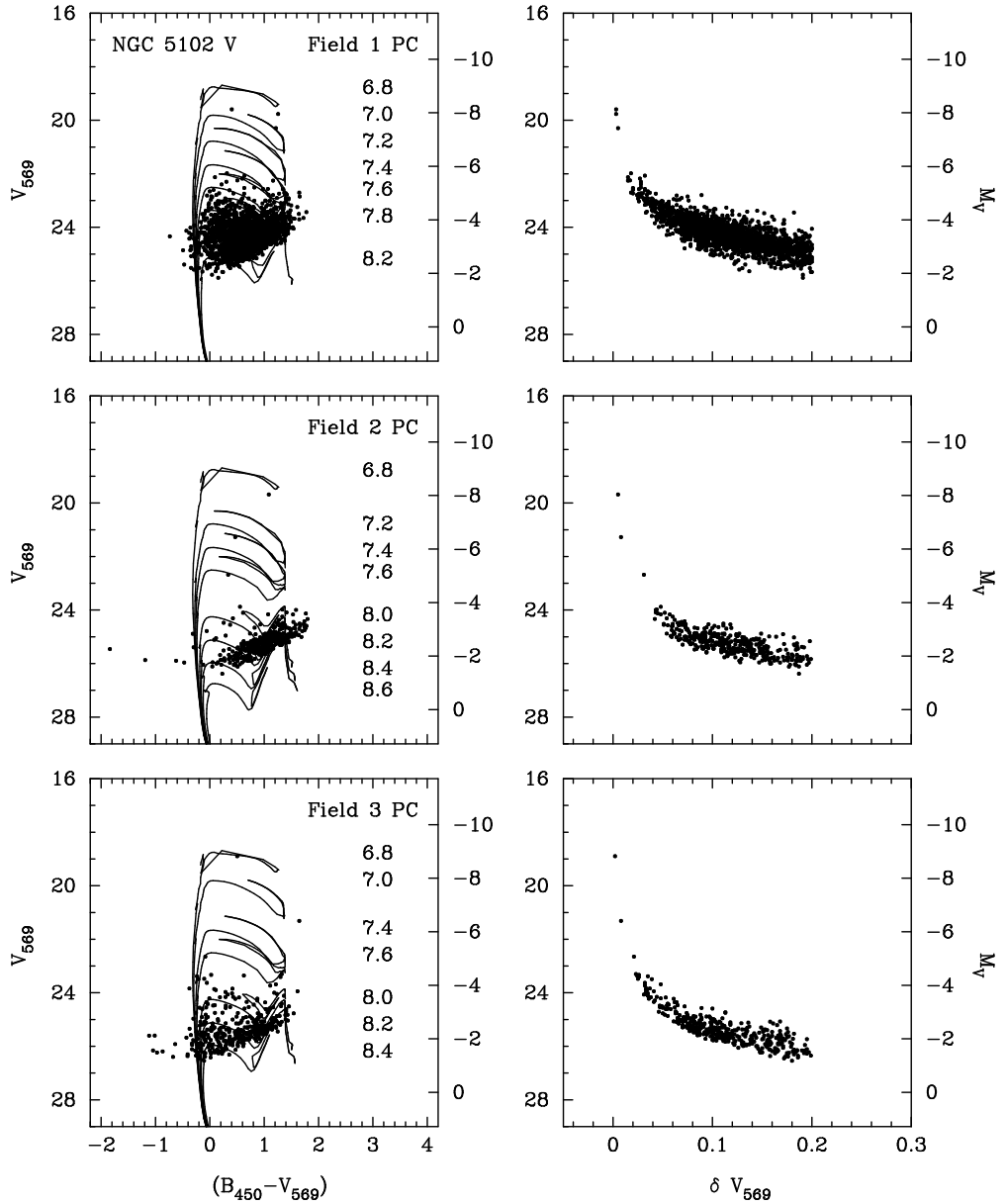

Fig. 8.— Left panel shows colour-magnitude data in the V- band for the three fields of NGC 5102. Overlaid on the data are $z = 0.02$ Padova isochrones with their log(age). The Galactic extinction correction has been applied. The right panel shows the associated photometric errors.

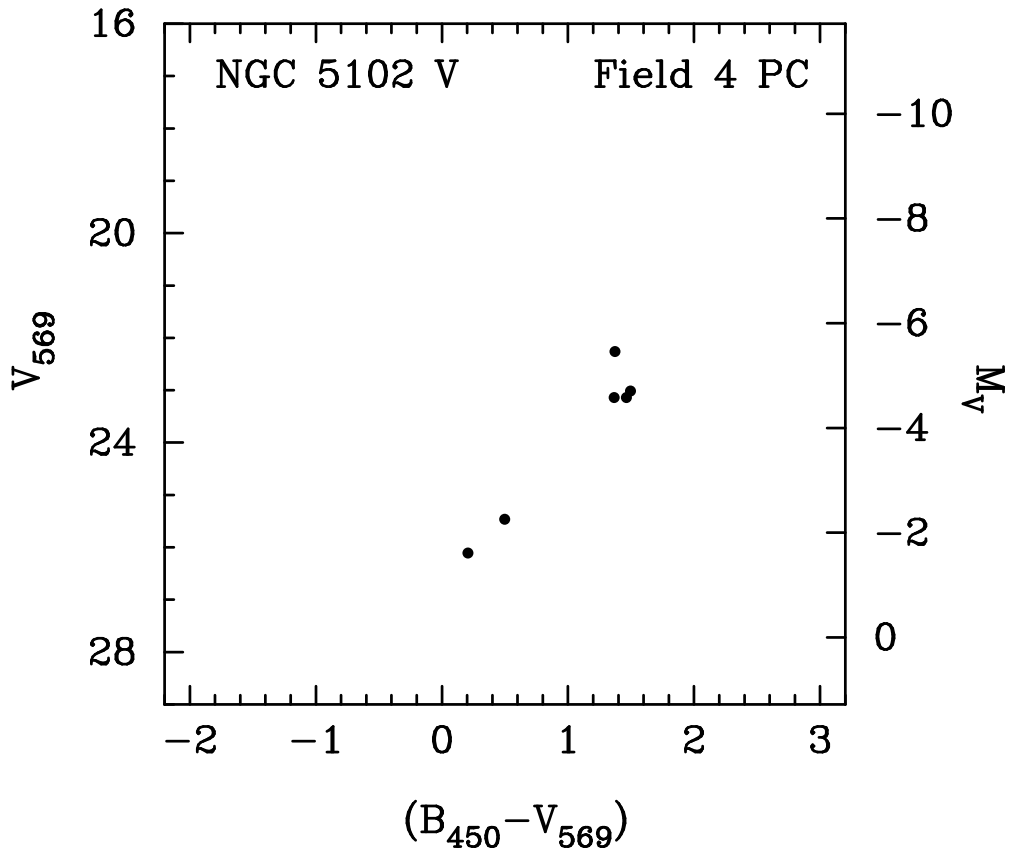

Fig. 9.— Colour-magnitude data in the V-band for the background field (field 4). We note that contamination from background stars is not a problem.

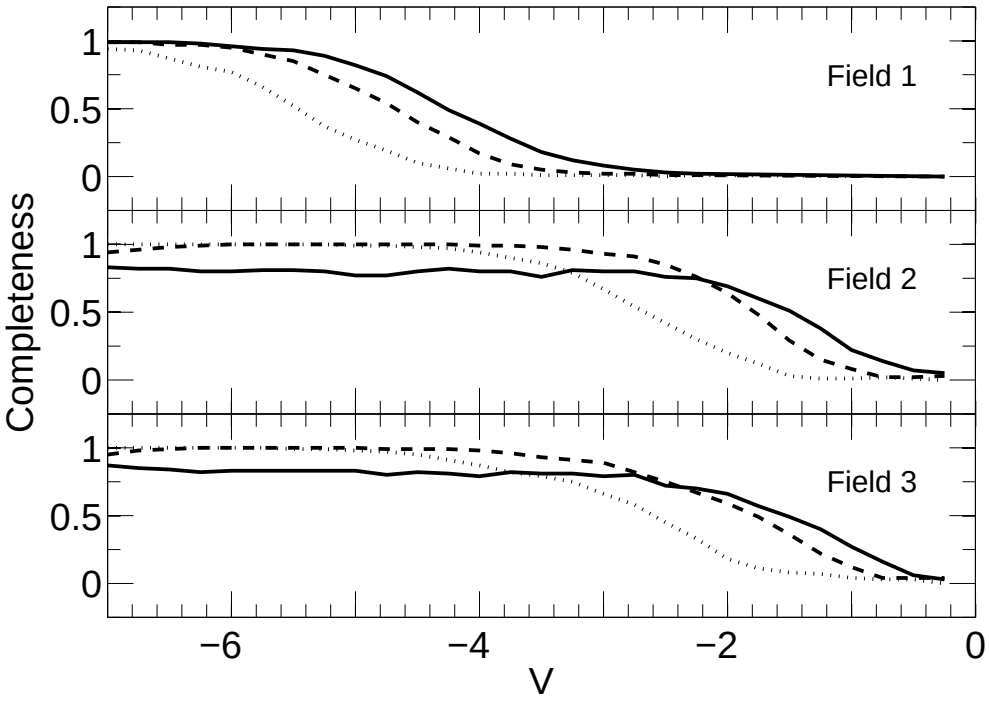

Fig. 10.— Completeness vs. absolute magnitude as a function of colour for the three fields in the V- band. We see a clear dependence on colour. As expected, the inner field (F1) is more crowded than the outer fields (F2 and F3). Solid line is for $(B-V) \leq 0$, dashed line is for $0 \leq (B-V) \leq 1$, and dotted line is for $(B-V) \geq 2$.

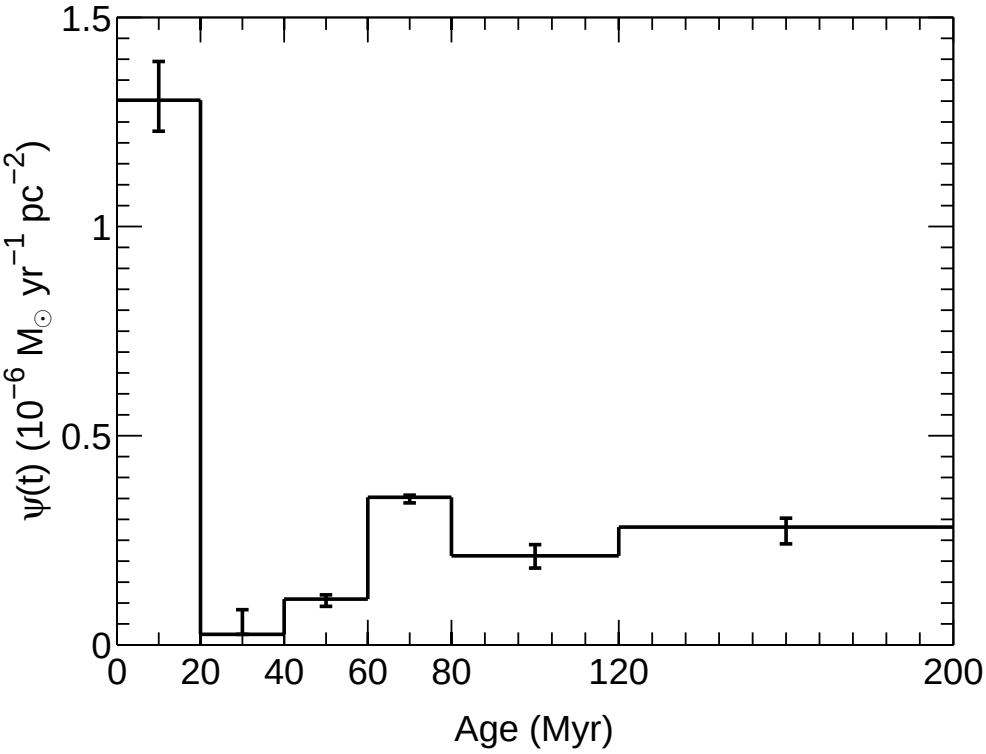

Fig. 11.— SFH of the central field (F1). The bright background of the central field means that it is not possible to probe the SFH older than 200 Myr. Here, we can see what appears to be a relatively high star formation rate over the past 20 Myr. The star formation rates shown here (and in Figures 13 and 15) are per unit area projected on the sky.

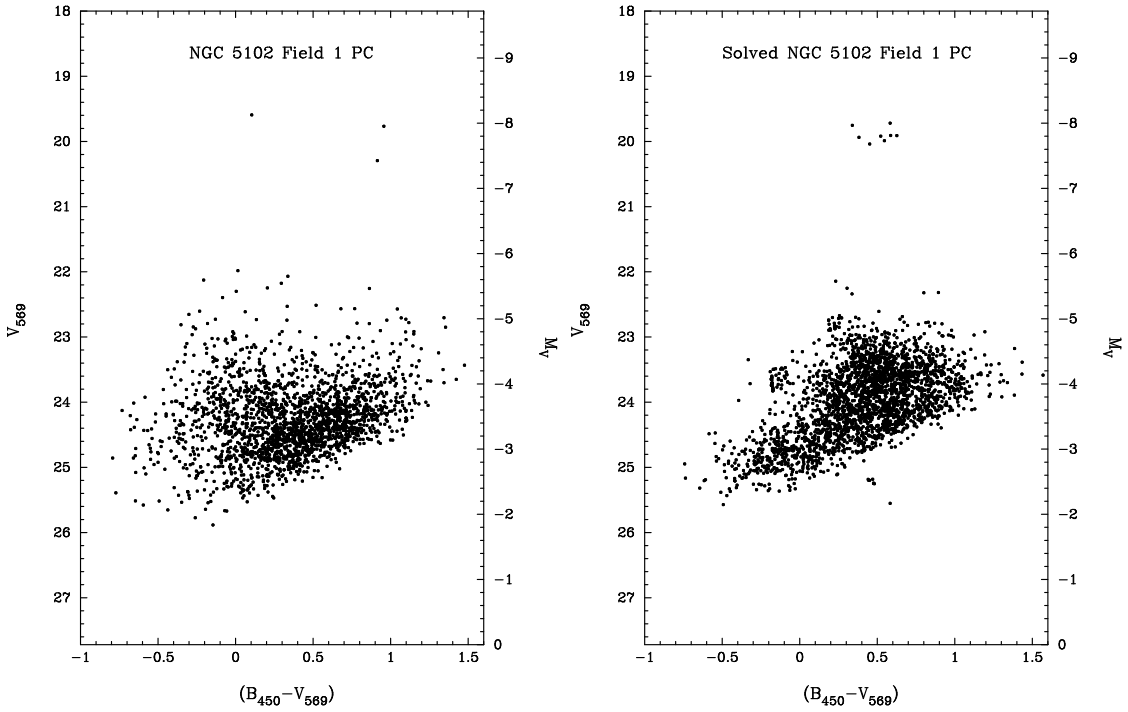

Fig. 12.— Observed CMD and solved CMD for the central field (F1).

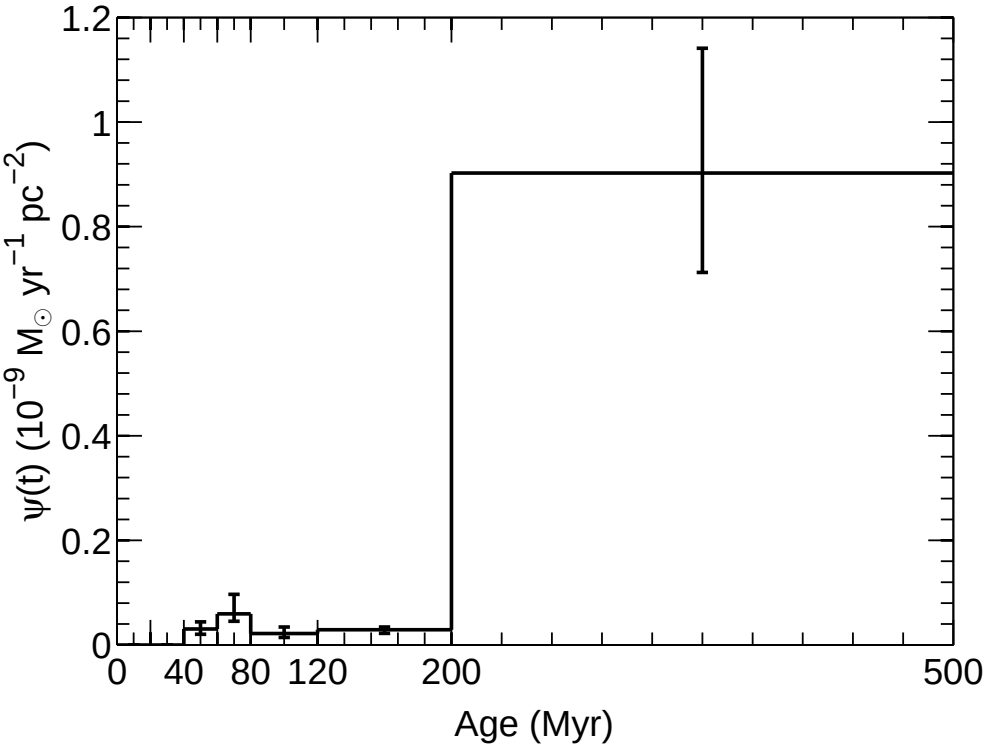

Fig. 13.— SFH of the intermediate field (F2). A decline in the star formation is seen from about 0.5 Gyr then, the past 200 Myr appear to have been quiescent.

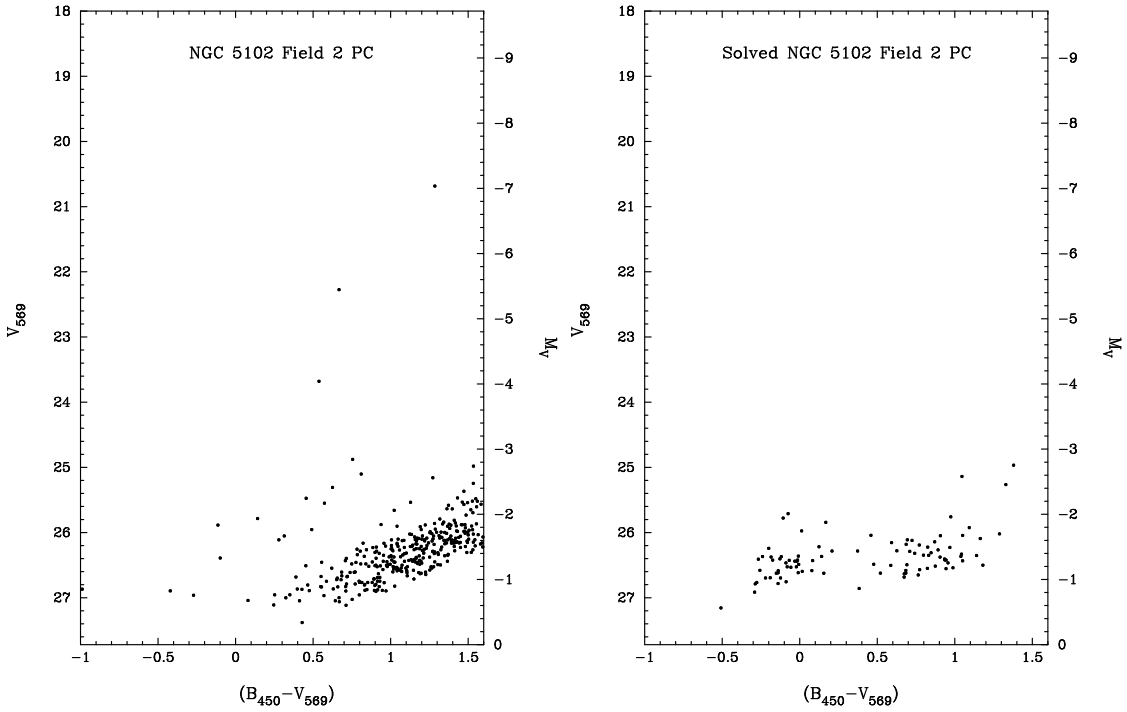

Fig. 14.— Observed CMD and solved CMD for the intermediate field (F2).

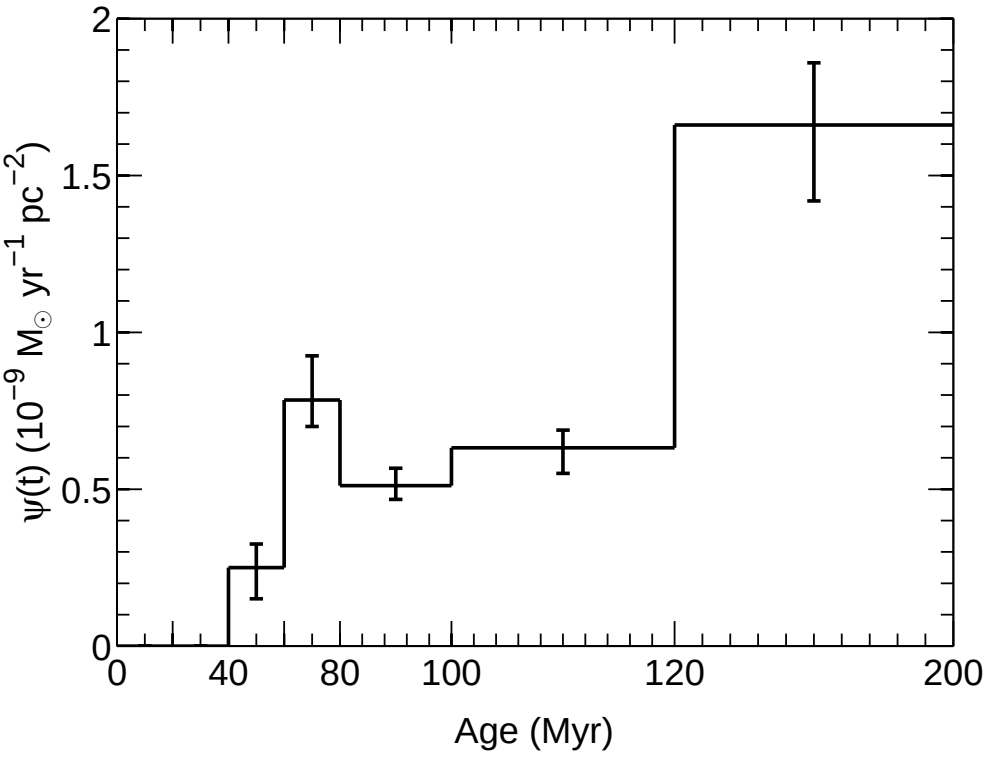

Fig. 15.— SFH of the disk field (F3). The star formation rate declined smoothly from about 200 Myr ago, and has been quiescent over the past 40 Myr.

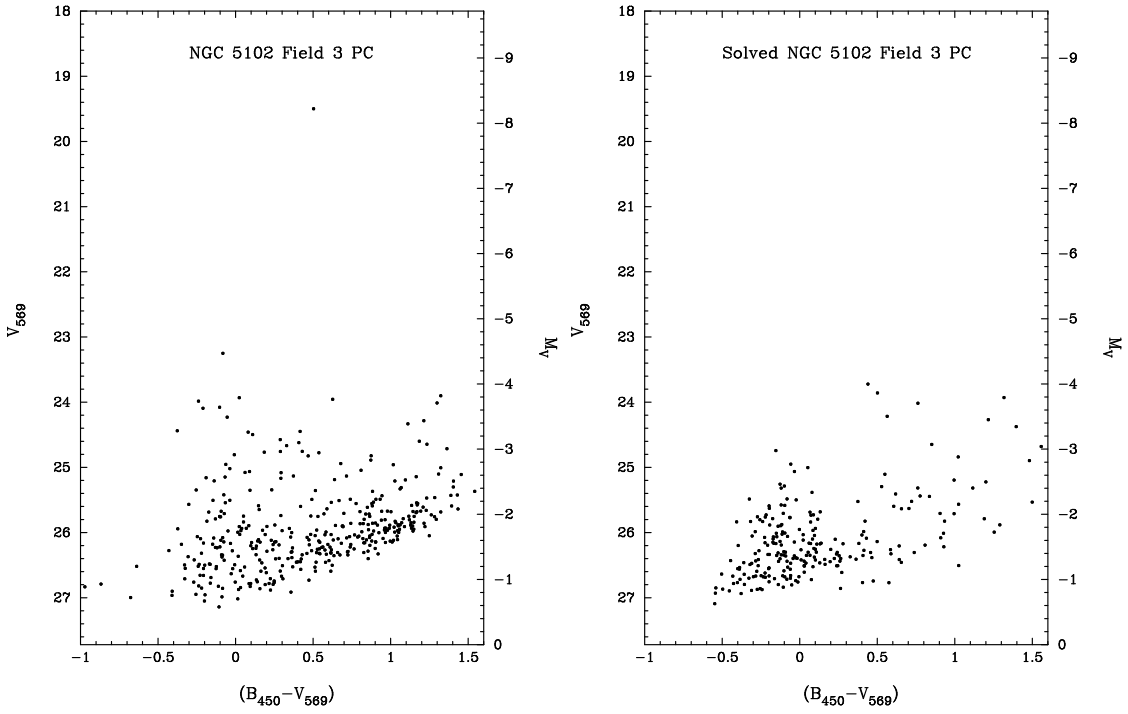

Fig. 16.— Observed CMD and solved CMD for the disk field (F3).